

# The kinetics of precipitation in Al-Mg and Al-Mg-Cu alloy

## Kinetika izločanja v zlitinah Al-Mg in Al-Mg-Cu

MAJA VONČINA<sup>1</sup>, PRIMOŽ MRVAR<sup>1</sup>, FRANC ZUPANIČ<sup>2</sup>, JOŽEF MEDVED<sup>1</sup>

<sup>1</sup>University of Ljubljana, Faculty of Natural Sciences and Engineering, Department of materials and metallurgy, Aškerčeva cesta 12, SI-1000 Ljubljana, Slovenia;

E-mail: maja.voncina@ntf.uni-lj.si, primoz.mrvar@ntf.uni-lj.si, jozef.medved@ntf.uni-lj.si

<sup>2</sup> University of Maribor, Faculty for Mechanical Engineering, University Center for Electron Microscopy, Smetanova ulica 17, 2000 Maribor, Slovenia; E-mail: franc.zupanic@uni-mb.si

**Received:** November 12, 2007

**Accepted:** December 18, 2007

**Abstract:** Aluminium alloys usually contain many alloying elements which form many phases. However, most of the heat-treatable alloys contain combinations of magnesium with one or more of the elements such as copper, silicon and zinc. In this work a triple simple thermal analysis (TETA) was used in order to achieve three different cooling rates and consequently three different stages of supersaturated solid solution. In addition melt spinning was used to obtain highly supersaturated solid solution. The course of equilibrium solidification of the alloys was calculated using the computer simulation (Thermo-Calc). To pursue the sequence of precipitation of hardening precipitates the differential scanning calorimetry (DSC) was used enabling determination of precipitation energy and the temperature of precipitation of precipitates from supersaturated solid solution. Scanning electron microscopy (SEM) and energy dispersive spectroscopy (EDS) was used to determine the phases formed during solidification. Using the DSC method the kinetics of precipitation from supersaturated solid solution in our case in AlMg7.5 and AlMg3Cu can be followed very precisely. The precipitation kinetics is related to increasing tendency for energy relaxation on heating DSC curve, and is enhanced with strongly supersaturated solid solutions. If the portion of the precipitation energy is calculated, it can be evident that, in the AlMg7.5 alloy, it increases with the increasing supersaturation. In the AlMg3Cu alloy the precipitation energy also increases from 0.8 % in specimen that was cooled in MC1 to 1.6 % in specimen that was rapidly solidified.

**Izvleček:** Aluminijeve zlitine običajno vsebujejo veliko zlitinskih elementov, zato imajo v mikrostrukturi več faz. Večina topotno utrjevalnih aluminijevih zlitin vsebuje kombinacijo magnezija z enim ali več elementi, kot so baker, silicij in cink. V tem delu je bila, za dosego različnih stanj prenasičene trdne raztopine, izvedena trojna enostavna termična analiza (TETA), pri čemer so bile dosežene tri različne ohlajevalne hitrosti ter posledično tri različne

prenasičene trdne raztopine. Z napravo za hitro strjevanje (Melt Spinner) pa je bila dosežena najbolj prenasičena trdna raztopina. Potek ravnotežnega strjevanja je bil določen z računalniško simulacijo Thermo-Calc. Za zasledovanje zaporedja izločanja utrijevalnih izločkov je bila uporabljena simultana termična analiza (STA) in sicer diferenčna vrstična kalorimetrija (DSC), s katero so bile določene energije izločanja ter temperature izločanja izločkov iz različnih prenasičenih trdnih raztopin. S pomočjo elektronske mikroskopije (SEM) ter energijsko disperzijске spektroskopije (EDS) so bili določeni tipi nastalih izločkov. Ob uporabi DSC metode je omogočeno izredno natančno zasledovanje kinetike izločanja iz prenasičene trdne raztopine, v našem primeru v zlitini AlMg<sub>7,5</sub> in AlMg<sub>3</sub>Cu. Kinetika izločanja je razvidna iz povečevanja sproščene energije izločanja, ki pa s se povečano prenasičenostjo samo še povečuje. Pri izračunu deleža sproščene energije je opaziti, da energija izločanja s prenasičenostjo v zlitini AlMg<sub>7,5</sub> naraste. Pri zlitini AlMg<sub>3</sub>Cu energija izločanja prav tako naraste od 0,8 % v vzorcu predhodno ohlajanem v MC1 na 1,6 % v vzorcu predhodno ohljenem na Melt Spinnerju.

**Key words:** Al-Mg alloy, Al-Mg-Cu alloy, thermal analysis, differential scanning calorimetry (DSC), precipitation kinetics

**Ključne besede:** zlitina Al-Mg, zlitina Al-Mg-Cu, termična analiza, diferenčna vrstična kalorimetrija (DSC), kinetika izločanja

## INTRODUCTION

Al-Mg and Al-Mg-Cu alloys are usually strengthened by nanoparticles that precipitate from a supersaturated solid solution. Nevertheless, most of the heat-treatable alloys contain combinations of magnesium with one or more of the elements like copper, silicon and zinc. Characteristically, even a small amount of magnesium in concert with these elements accelerates and accentuates precipitation hardening. The structural changes, which are formed as a result of precipitation of atoms from solid solution, have extraordinary technological and industrial meaning.

The majority of heat-treatable aluminium alloy systems exhibit multistage precipitation and undergo accompanying strength

changes. Multiple alloying additions of elements employed in commercial alloys are strictly functional and with different heat treatments serve to provide many different combinations of properties<sup>[1]</sup>.

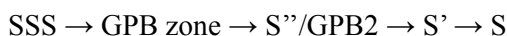
Heat treatment to increase strength of aluminium alloys is a three-step process:

1. Solution heat treatment: dissolution of soluble phases.
2. Quenching: development of supersaturated solid solution.
3. Age hardening: precipitation of solute atoms either at room temperature (natural aging) or elevated temperature (artificial aging)<sup>[1]</sup>.

The classical Al-Mg alloy is typically used for car body construction, where certain problems can occur during the paint-bak-

ing treatment, due to the softening of Al-Mg parts. The undesirable softening can be overcome either by using precipitation hardening at paint-baking temperatures (160-180 °C) either with small additions of copper, which makes the alloys precipitation hardenable during paint-baking treatment<sup>[1]</sup>.

During aging of Al-Mg-Cu alloy the precipitation takes place in following sequence:



SSS stands for supersaturated solid solution and GPB for Guinier-Preston-Bagaryatsky<sup>[1,2]</sup>. The transition phases (GPB zone, S'', S') are formed because they have a lower activation energy barrier for nucleation than the equilibrium phases. S-phase prefers to nucleate on defects, therefore dislocations and dislocation loops are the favoured nucleation sites<sup>[1]</sup>.

In this work we investigated the precipitation kinetics from different supersaturated solid solutions in two alloys: binary AlMg7.5 and ternary AlMg3Cu. The latter alloy was chosen in order to determine the influence of copper on precipitation kinetics. The most important goals were to determine energies and temperatures of precipitation.

## EXPERIMENTAL

The investigated AlMg7.5 and AlMg3Cu alloys were made out of pure electrolytic

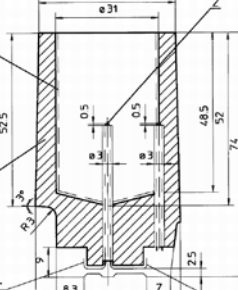
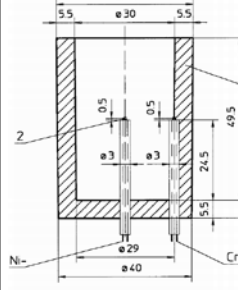
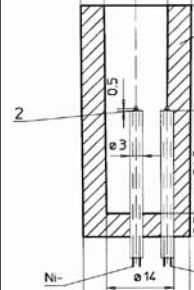
aluminium (99.98 %), pure magnesium and pure copper. Alloys were melted in graphite crucible and cast into three measuring cells (Table 1) of triple simple thermal analysis (TETA)<sup>[1]</sup> with a purpose to obtain three different supersaturated solid solutions.

These alloys were also casted on the device for rapid solidification (Melt Spinner). The process is schematically presented in Figure 1. During melt spinning the liquid metal is cast upon a fast rotating copper wheel. A stable melt puddle appears when the wheel's velocity attains the critical point (up to 35 m/s). The thickness, width and length of ribbons depend on the wheel's velocity, substrate material, melt superheat, injection pressure, nozzle diameter and the distance between the nozzle and the wheel. Consequently, the ribbons with a thickness range of 10 µm to a few mm, and with width range of 1 to 12 mm at solidification rate from 10<sup>2</sup> to 10<sup>6</sup> K/s are produced<sup>[1]</sup>.

After TETA the specimens were chemically analysed. In order to determine the intensity and the energy of precipitation from various supersaturated solutions the differential scanning calorimetry (DSC) of simultaneous thermal analysis (STA) Jupiter 449c of NETZSCH enterprise was used.

With a purpose to determine phase formed during solidification in investigated alloys the Scanning Electron Microscopy (SEM) with EDS analyser (Sirion 400 NC equipped with INCA 350) was used.

**Table 1.** Measuring cells of triple simple thermal analysis  
**Tabela 1.** Merilne celice trojne enostavne termične analize

Figure	 <p>Technical drawing of casting MC1. The casting has a height of 74 mm and a base diameter of Ø435 mm. It features a central vertical rib with a thickness of 3 mm. The top section has a height of 52.5 mm and a horizontal width of Ø41 mm. The side walls have a thickness of 31 mm. Material layers include Ni- at the base, CrNi+ in the center, and a top layer with a thickness of 3 mm. Key dimensions: height 74, base dia Ø435, top width Ø41, side wall thickness 31, rib thickness 3, base thickness 25, top height 52.5.</p>	 <p>Technical drawing of casting MC2. The casting has a height of 69.5 mm and a base diameter of Ø40 mm. It features a central vertical rib with a thickness of 3 mm. The top section has a height of 24.5 mm and a horizontal width of Ø30 mm. The side walls have a thickness of 30 mm. Material layers include Ni- at the base, CrNi+ in the center, and a top layer with a thickness of 3 mm. Key dimensions: height 69.5, base dia Ø40, top width Ø30, side wall thickness 30, rib thickness 3, base thickness 24.5.</p>	 <p>Technical drawing of casting MC3. The casting has a height of 49.5 mm and a base diameter of Ø25 mm. It features a central vertical rib with a thickness of 3 mm. The top section has a height of 24.5 mm and a horizontal width of Ø26 mm. The side walls have a thickness of 15 mm. Material layers include Ni- at the base, CrNi+ in the center, and a top layer with a thickness of 3 mm. Key dimensions: height 49.5, base dia Ø25, top width Ø26, side wall thickness 15, rib thickness 3, base thickness 24.5.</p>
Material	Cronning sand	Gray cast iron	Gray cast iron
Designation	MC1	MC2	MC3

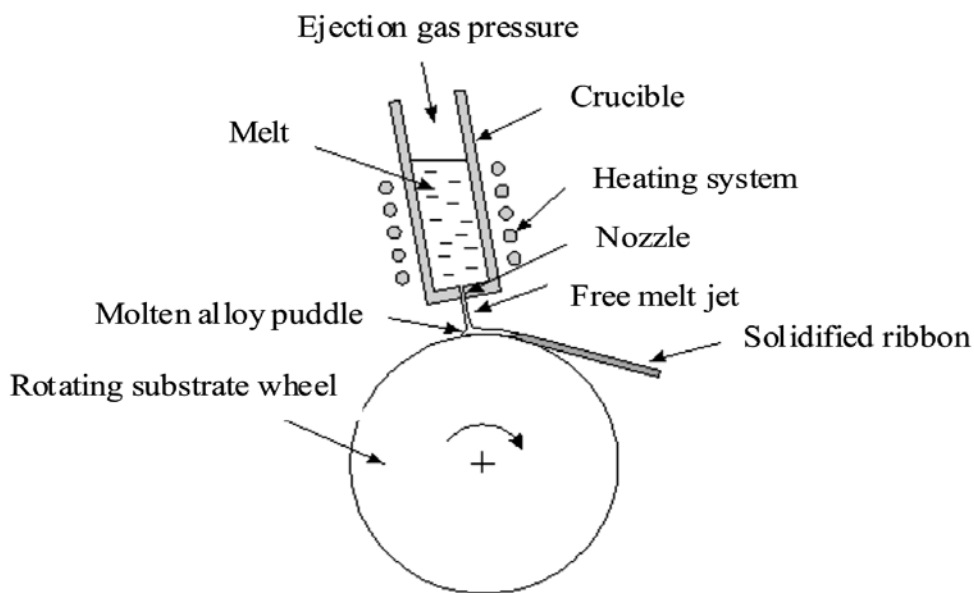


**Figure 1.** Scheme of a free jet melt spinner<sup>[7]</sup>

**Table 2.** Chemical composition of the investigated alloys**Tabela 2.** Kemijska sestava preiskovanih zlitin

Element/mass. %								
Alloy	Cu	Zn	Mg	Mn	Si	Ti	Fe	Al
<b>AlMg7.5</b>	0.00061	0.0114	7.572	0.0035	0.0534	0.00012	0.1417	rest
<b>AlMg3Cu</b>	0.8451	0.0107	3.253	0.0030	0.0547	0.00002	0.1932	rest

**Table 3.** The course of equilibrium solidification calculated using Thermo-Calc program**Tabela 3.** Potek ravnotežnega strjevanja, izračunanega s programom Thermo-Calc

AlMg7.5		AlMg3Cu	
Temp. /°C	Reaction	Temp. /°C	Reaction
620	$L \rightarrow \alpha_{Al}$	640	$L \rightarrow \alpha_{Al}$
606	$L \rightarrow \alpha_{Al} + Al_{13}Fe_4$	622	$L \rightarrow \alpha_{Al} + Al_{13}Fe_4$
546	$L \rightarrow \alpha_{Al} + Mg_2Si$	550	$\alpha_{Al} \rightarrow Mg_2Si$
314	$\alpha_{Al} \rightarrow Al_3Mg$	396	$\alpha_{Al} \rightarrow Al_xMg_yCu_z$
230	$\alpha_{Al} \rightarrow Al_{15}Mg_{10}Cu$	293	$\alpha_{Al} \rightarrow Al_{15}Mg_{10}Cu$
156	$\alpha_{Al} \rightarrow Al_6Mn$	253	$\alpha_{Al} + Al_xMg_yCu_z \rightarrow Al_{15}Mg_{10}Cu$
50	$\alpha_{Al} \rightarrow Al_5Ti$	111	$\alpha_{Al} \rightarrow Al_6Mn$
		9	$\alpha_{Al} \rightarrow Al_5Ti$

## RESULTS AND DISCUSSION

The chemical composition of the investigated alloys is presented in Table 2.

In Table 3 the course of equilibrium solidification of the alloys was calculated using the computer application Thermo-Calc. Equilibrium phase diagrams are shown in Figure 2. From Table 3 and Figure 2 the temperature of primary solidification, eutectic solidification and precipitation at equilibrium conditions can be determined.

The sequence of solidification can be influenced by concentration of alloying elements (i. e. chemical composition).

From the cooling curves in Figure 3 the temperature of primary solidification, solidification of eutectic and the temperature of precipitation in the investigated alloys are evident. With the increasing cooling rate the peaks in differential cooling curve decreases. The alloy is now supersaturated with magnesium in case of AlMg7.5 alloy and magnesium and copper in case of AlMg3Cu alloy. The characteristic temperatures are also changing in dependence of the type and concentration of alloying elements.

The solidification of AlMg7.5 and AlMg3Cu alloys is presented in Figure

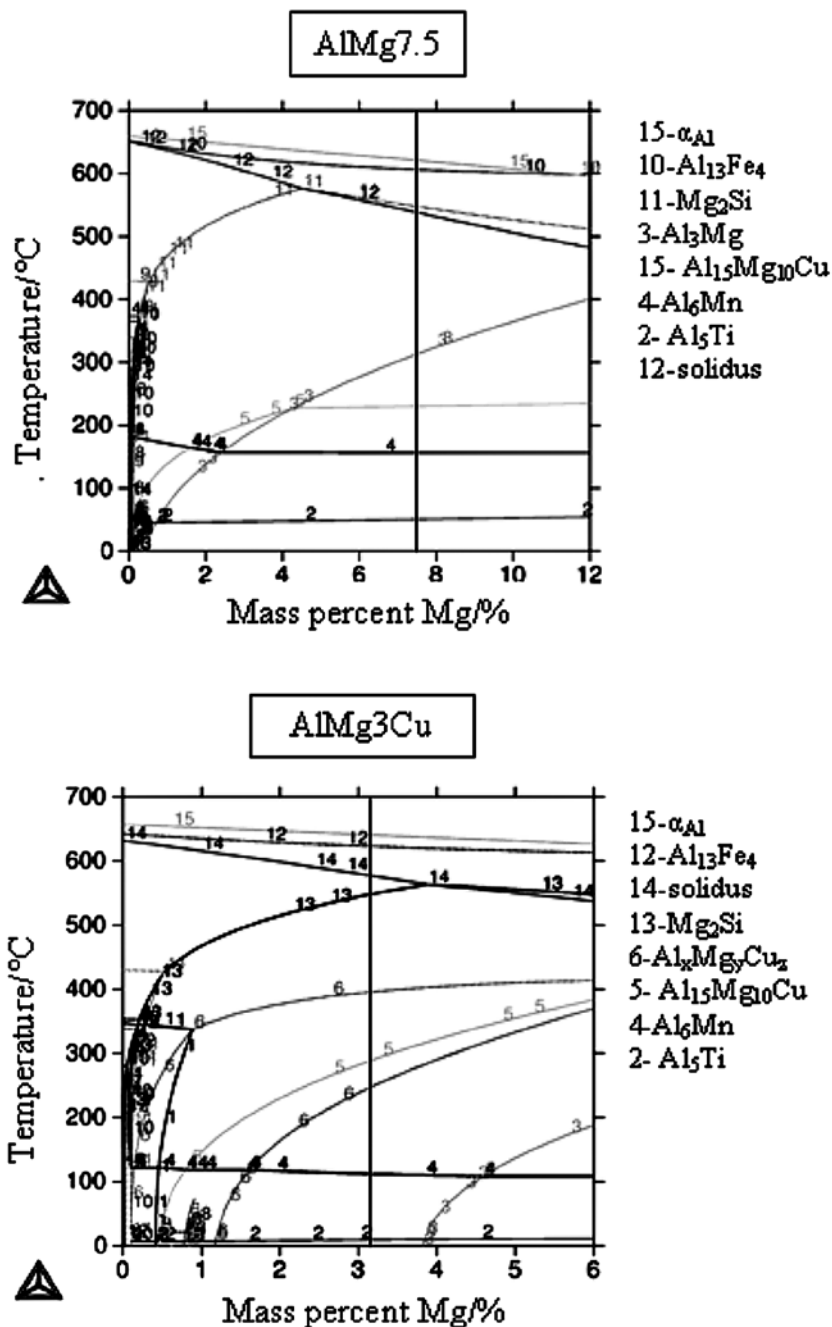


**Figure 2.** Isopleth equilibrium phase diagram of AlMg7.5 and AlMg3Cu alloy  
**Slika 2.** Izopletni ravnotežni fazni diagrami zlitin AlMg7,5 ter AlMg3Cu

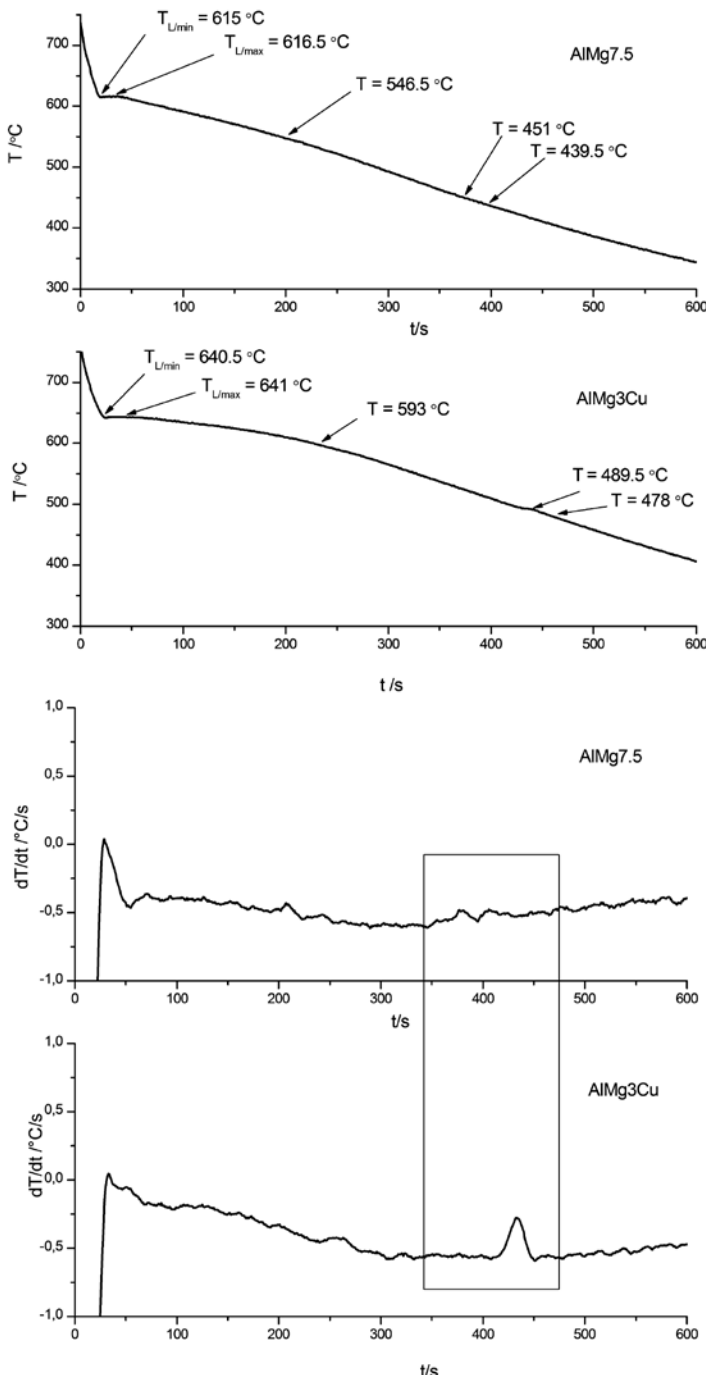


**Figure 3.** Cooling curves and differential cooling curves of investigated alloys  
**Slika 3.** Ohlajevalne in diferencirane ohlajevalne krivulje preiskovanih zlitin

**Table 4.** The energy and temperature of solidification and melting of specific phases in investigated alloys

**Tabela 4.** Energije in temperature strjevanja in taljenja posameznih faz pri preiskovanih zlitinah

AlMg7.5 – MC1							
DSC - heating			DSC - cooling				
Temp. /°C	Reaction	Energy (x0.9513 J/g)	Temp. /°C	Reaction	Energy (x0.9513 J/g)		
576.1	$L \rightarrow \alpha_{Al}$	-135.47	609.4	$L \rightarrow \alpha_{Al}$	161.15		
529.7	$L \rightarrow \alpha_{Al} + Al_{13}Fe_4$		550.5	$L \rightarrow \alpha_{Al} + Al_{13}Fe_4$			
447.1	$L \rightarrow \alpha_{Al} + Mg, Si$		521.5	$L \rightarrow \alpha_{Al} + Mg, Si$			
308.6	$\alpha_{Al} \rightarrow AlMg$		0.07				
AlMg7.5 – MC2							
606.5	$L \rightarrow \alpha_{Al}$	-262.56	612.4	$L \rightarrow \alpha_{Al}$	275.40		
532.2	$L \rightarrow \alpha_{Al} + Al_{13}Fe_4$		566.7	$L \rightarrow \alpha_{Al} + Al_{13}Fe_4$			
447.2	$L \rightarrow \alpha_{Al} + Mg, Si$		551.1	$L \rightarrow \alpha_{Al} + Mg, Si$			
279.5	$\alpha_{Al} \rightarrow AlMg$		0.47				
AlMg7.5 – MC3							
574.0	$L \rightarrow \alpha_{Al}$	-287.96	609	$L \rightarrow \alpha_{Al}$	280.44		
532.7	$L \rightarrow \alpha_{Al} + Al_{13}Fe_4$		545	$L \rightarrow \alpha_{Al} + Al_{13}Fe_4$			
336.1	$\alpha_{Al} \rightarrow AlMg$		-6.63	$L \rightarrow \alpha_{Al} + Mg, Si$			
AlMg7.5 – rapid solidification							
556.1	$L \rightarrow \alpha_{Al}$	-221.94	618.7	$L \rightarrow \alpha_{Al}$	220.04		
536.1	$L \rightarrow \alpha_{Al} + Al_{13}Fe_4$		565.4	$L \rightarrow \alpha_{Al} + Al_{13}Fe_4$			
310.0	$\alpha_{Al} \rightarrow AlMg$		-0.89	$L \rightarrow \alpha_{Al} + Mg, Si$			
AlMg3Cu – MC1							
DSC - heating			DSC - cooling				
Temp. /°C	Reaction	Energy (x0.9513 J/g)	Temp. /°C	Reaction	Energy (x0.9513 J/g)		
575.5	$L \rightarrow \alpha_{Al}$	-205.10	633.7	$L \rightarrow \alpha_{Al}$	211.66		
508.2	$L \rightarrow \alpha_{Al} + Mg, Si$	-3.521	580.3	$L \rightarrow \alpha_{Al} + Al_{13}Fe_4$			
293.4	$\alpha_{Al} \rightarrow Al_xMg_yCu_z$	1.708	489.8	$L \rightarrow \alpha_{Al} + Mg, Si$			
AlMg3Cu – MC2							
577.5	$L \rightarrow \alpha_{Al}$	-207.38	633.0	$L \rightarrow \alpha_{Al}$	211.09		
511.3	$L \rightarrow \alpha_{Al} + Mg, Si$	-2.04	576.7	$L \rightarrow \alpha_{Al} + Al_{13}Fe_4$			
254.5	$\alpha_{Al} \rightarrow Al_xMg_yCu_z$	2.19	477.7	$L \rightarrow \alpha_{Al} + Mg, Si$			
AlMg3Cu – MC3							
576.3	$L \rightarrow \alpha_{Al}$	-303.75	636.0	$L \rightarrow \alpha_{Al}$	303.56		
510.0	$L \rightarrow \alpha_{Al} + Mg, Si$	-1.88	583.0	$L \rightarrow \alpha_{Al} + Al_{13}Fe_4$			
251.4	$\alpha_{Al} \rightarrow Al_xMg_yCu_z$	1.38	484.0	$L \rightarrow \alpha_{Al} + Mg, Si$			
AlMg3Cu – rapid solidification							
574.4	$L \rightarrow \alpha_{Al}$	-260.09	635.9	$L \rightarrow \alpha_{Al}$	256.37		
246.5	$\alpha_{Al} \rightarrow Al_xMg_yCu_z$	4.28	592.6	$L \rightarrow \alpha_{Al} + Al_{13}Fe_4$			
			476.6	$L \rightarrow \alpha_{Al} + Mg, Si$			

\* 0.9513 is a correction factor of STA machine for aluminium alloys at current conditions.

3. The primary solidification at the alloy AlMg7.5 occurred at 615 °C or 616.5 °C. The undercooling was 5 °C and the recalescence 1.5 °C. The eutectic ( $\alpha_{\text{Al}} + \text{Al}_{13}\text{Fe}_4$ ) solidified at 546.5 °C, eutectic ( $\alpha_{\text{Al}} + \text{Mg}_2\text{Si}$ ) solidified at 451 °C. These characteristic temperatures are somewhat lower than theoretical ones, because of the unequilibrium solidification of the alloy.

AlMg3Cu alloy started to solidify at 640.5 °C or 641 °C (Figure 3). The solidification of eutectic ( $\alpha_{\text{Al}} + \text{Al}_{13}\text{Fe}_4$ ) started at temperature 593 °C. Eutectic ( $\alpha_{\text{Al}} + \text{Mg}_2\text{Si}$ ) solidified at 489.5 °C. As mentioned above, these temperatures result differ from the theoretical ones because of the unequilibrium solidification.

At higher cooling rates the characteristic temperatures of primary and eutectic solidification move to lower temperatures.

From DSC curves on Figure 4 and 5 and from Table 4 the energy of formation and melting of specific phases are determined. The temperature where the solidification of specific phase starts (in cooling DSC curve) and temperature where the solidification of specific phase ends (in heating DSC curve) are also determined. Only heating DSC curves of investigated alloys are presented.

In AlMg7.5 alloy some changes between the heating DSC curves can be seen. These are the consequences of different cooling rates (Figure 4). It is obvious that the precipitation in specimens is intensified with higher supersaturation of Mg in solid solution; i.e. in specimens cooled with higher cooling rates. During reheating magnesium

is precipitated from  $\alpha_{\text{Al}}$  in a form of  $\text{Al}_x\text{Mg}_y$  precipitates. In Figure 5 the precipitation kinetics can be even clearly seen. Namely, there is a stronger tendency for energy relaxation on heating DSC curves in samples previously cooled with higher rates and a fact that the solid solution in Al-Mg-Cu alloy is more supersaturated solid solutions. At higher magnification it can be clearly seen, that the precipitation temperature decreases with the increasing supersaturation. The energy of precipitation also increases with the increasing supersaturation of the alloy. Here the precipitation of  $\text{Al}_x\text{Mg}_y\text{Cu}_z$  precipitates took place within the primary crystals of  $\alpha_{\text{Al}}$ . In addition, if the portion of the energy for the precipitation is calculated it can be evident, that the fraction of the precipitation energy is increasing with the increasing supersaturation, so the portion of the precipitates in the microstructure increases. The portion of precipitation energy in AlMg7.5 alloy increases from 0.05 % in specimen that was cooled in MC1 to 0.18 % in specimen that was cooled in MC2 and to 0.3 % at specimen that was rapidly solidified. In the AlMg3Cu alloy the precipitation energy increases from 0.8 % in specimen that was cooled in MC1 to 1.0 % in specimen that was cooled in MC2 and to 1.6 % in specimen that was rapidly solidified. As already mentioned the copper in the alloy accelerates and accentuates precipitation hardening. That is evident from the fraction of precipitation energy in heating DSC curves of AlMg7.5 and AlMg3Cu alloys. The portion of precipitation is higher in AlMg3Cu alloy at each level of the supersaturation. The portion of precipitation energy was calculated as a portion from the total solidification energy (precipitation energy divided with the total

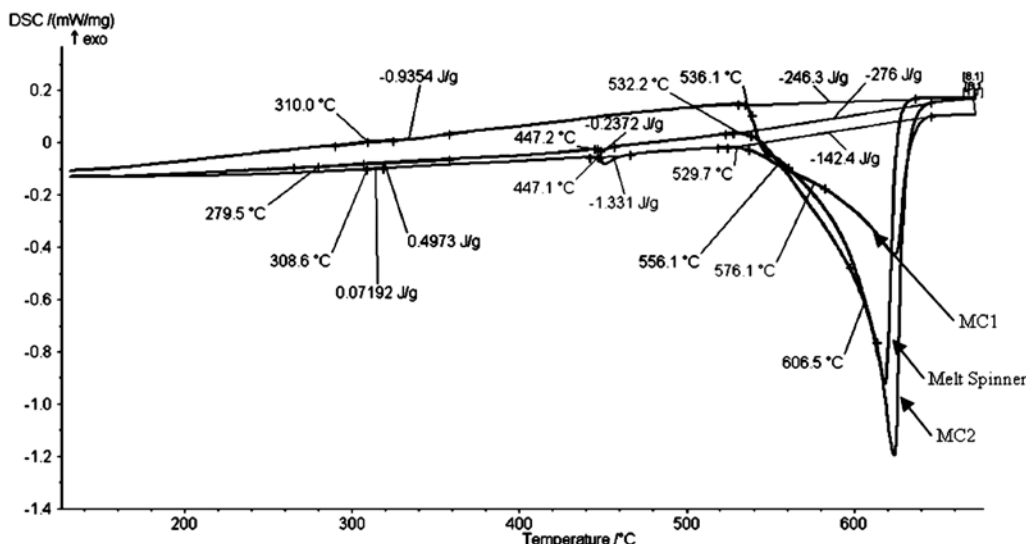


**Figure 4.** Heating DSC curves of specimens made of AlMg7.5 alloy: previously cooled in MC1, previously cooled in MC2 and previously cooled with Melt Spinner

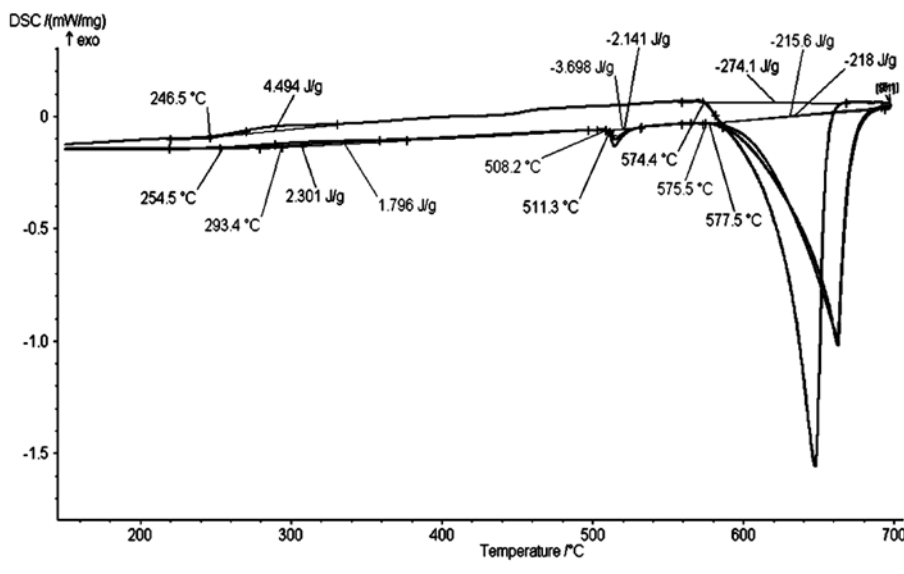
**Slika 4.** Segrevalne DSC krivulje vzorca iz zlitine AlMg7,5: predhodno ohlajene v MC1, predhodno ohlajene v MC2 in predhodno ohlajene na napravi Melt Spinner

solidification energy). Furthermore, when the specimen was cooled very quickly the melting of eutectics ( $\alpha_{\text{Al}} + \text{Al}_{13}\text{Fe}_4$ ) and ( $\alpha_{\text{Al}} + \text{Mg}_2\text{Si}$ ), and primary phase takes place in one step. On the other hand, when the cooling of the specimen was slow, the melting of eutectics ( $\alpha_{\text{Al}} + \text{Al}_{13}\text{Fe}_4$ ) and ( $\alpha_{\text{Al}} + \text{Mg}_2\text{Si}$ ), and primary phase takes place in two steps.

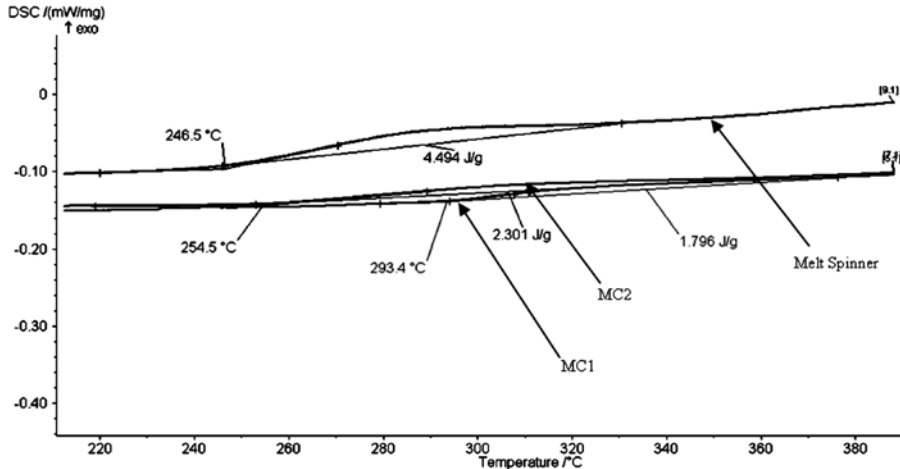
Using the scanning electron microscope and energy dispersive spectroscopy the microstructure constituents in all investigated alloys were analysed. In Figure 6 the microstructure of AlMg7.5 alloy with the

EDS analysis are presented. In the microstructure primary crystals of  $\alpha_{\text{Al}}$  and the eutectic ( $\alpha_{\text{Al}} + \text{Al}_{13}\text{Fe}_4$ ) are visible. When the specimen was ached in a diluted solution of HF acid for approximately 10 minutes also  $\text{Al}_3\text{Mg}_2$  precipitates become visible.

In the specimen AlMg3Cu in Figure 7 the primary crystals of  $\alpha_{\text{Al}}$  and the eutectic ( $\alpha_{\text{Al}} + \text{Al}_{13}\text{Fe}_4$ ) were determined. In the structure the phase on the basis of aluminium with some magnesium and copper were also determined, which did not correspond to stoichiometry that was described in literature<sup>[5]</sup>.



a)



b)

**Figure 5.** Heating DSC curves of specimens made of AlMg3Cu alloy: previously cooled in MC1, previously cooled in MC2 and previously cooled with Melt Spinner: whole heating curve (a) and heating curve at the precipitation (b)

**Slika 5.** Segrevalne DSC krivulje vzorca iz zlitine AlMg3Cu: predhodno ohlajene v MC1, predhodno ohlajene v MC2 in predhodno ohlajene na napravi Melt Spinner: celotna segrevalna krivulja (a) ter segrevalna krivulja pri izločanju (b)

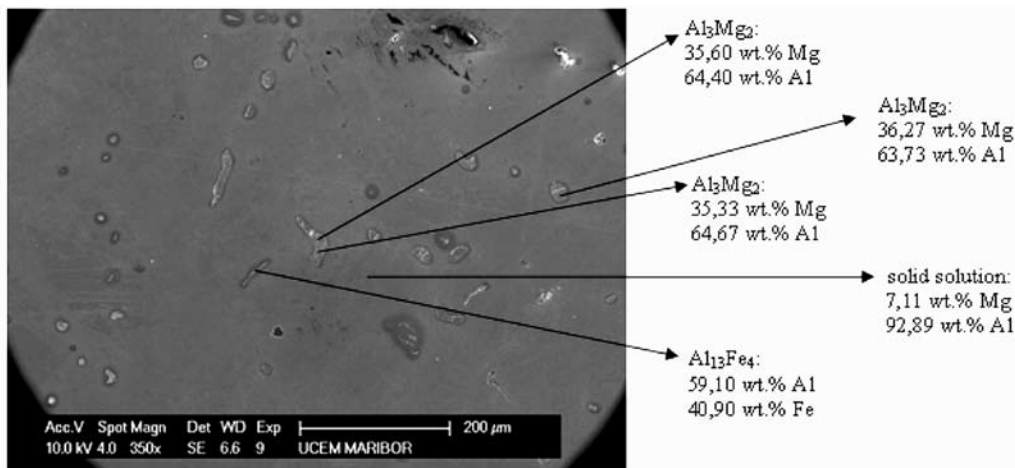


**Figure 6.** Secondary elektron image of AlMg7.5 alloy (SEM)  
**Slika 6.** SEM mikroposnetek zlitine AlMg7,5 (SEM)

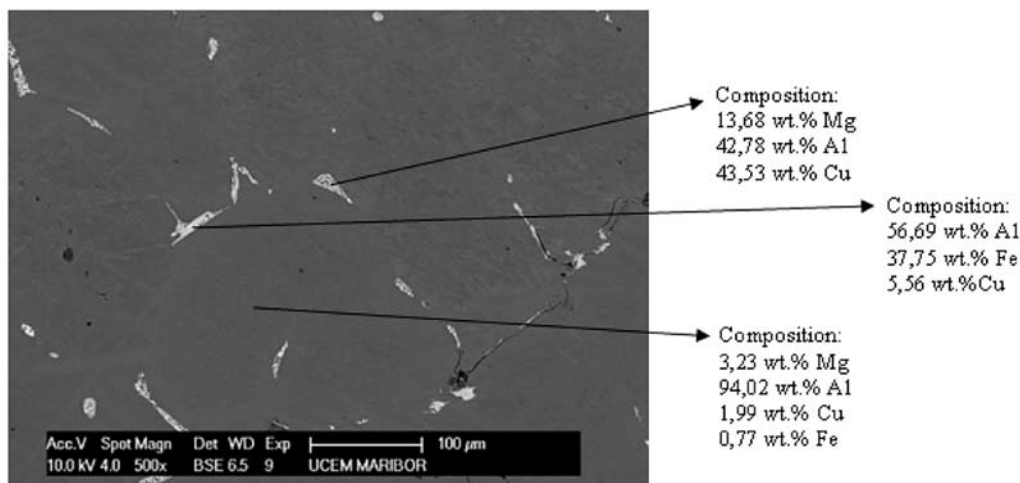


**Figure 7.** Secondary elektron image of AlMg3Cu alloy (SEM)  
**Slika 7.** SEM mikroposnetek zlitine AlMg3Cu (SEM)

## CONCLUSIONS

From the above presented results a few conclusions can be made:

- Using the DSC method the kinetics of precipitation from supersaturated solid solution in our case in AlMg7.5 and AlMg3Cu can be followed very precisely.
- The precipitation kinetics is related to increasing tendency for energy relaxation on heating DSC curve, and is enhanced with strongly supersaturated solid solutions.
- The temperature of precipitation decreases with the increasing supersaturation. The energy of precipitation also increases with the increasing supersaturation of solid solution. If the portion of the precipitation energy is calculated, it can be evident that, in the AlMg7.5 alloy, it increases with the increasing supersaturation from 0.05 % in specimen that was cooled in MC1 to 0.18 % in specimen that was cooled in MC2 and to 0.3 % at specimen that was rapidly solidified. In the AlMg3Cu alloy the precipitation energy increases from 0.8 % in specimen that was cooled in MC1 to 1.0 % in specimen that was cooled in MC2 and to 1.6 % in specimen that was rapidly solidified.
- When comparing the behaviour of both alloys, it becomes evident that copper in the alloy enhances the precipitation. The portion of precipitation was higher in AlMg3Cu alloy in each level of supersaturation. Consequently, more precipitates in the microstructure of the AlMg3Cu alloy can be expected.
- Microstructure constituents have been analysed. In specimens, primary crystals

of  $\alpha_{\text{Al}}$  and eutectic ( $\alpha_{\text{Al}} + \text{Al}_3\text{Fe}_4$ ) have been observed. In case of AlMg7.5 alloy the  $\text{Al}_3\text{Mg}_2$  precipitates were found. In case of AlMg3Cu alloy the precipitates on base of aluminium with some magnesium and copper were determined, which stoichiometry did not correspond to that described in literature<sup>[5]</sup>.

## POVZETEK

### Kinetika izločanja v zlitinah Al-Mg in Al-Mg-Cu

Aluminijeve zlitine običajno vsebujejo veliko zlitinskih elementov, zato imajo v mikrostrukturi več faz. Večina topotno utrjevalnih aluminijevih zlitin vsebujejo kombinacijo magnezija z enim ali več elementi, kot so baker, silicij in cink. Že majhna koncentracija magnezija v povezavi s temi elementi pospeši in poudari izločevalno utrjevanje. Strukturne spremembe, ki so posledica izločanja atomov iz trdne raztopine, so izrednega tehnološkega in industrijskega pomena.

Večino aluminijevih zlitin utrjujemo večstopenjsko. Dodajanje večjega števila zlitinskih elementov je nujno samo za funkcionalne namene ter za določene topotne obdelave ter tako omogočajo različne kombinacije lastnosti: fizikalne, mehanske, elektromehanske, ki so potrebne za različne aplikacije<sup>[1]</sup>.

Zlitine Al-Mg ter Al-Mg-Cu se utrjujejo z izločanjem nanodelcev iz prenasičene trdne raztopine. V tem delu smo za doseganje različnih stopenj prenasičenja trdne raztopine izvedli trojno enostavno termič-

no analizo (TETA), pri čemer so bile dosežene tri različne ohlajevalne hitrosti. S hitrim strjevanjem (Melt Spinner) pa je bila dosežena najbolj prenasičena trdna raztopina. Za zasledovanje zaporedja izločanja utrjevalnih izločkov je bila uporabljena simultana termična analiza (STA) in sicer diferenčna vrstična kalorimetrija (DSC), s katero so bile določene energije izločanja ter temperature izločanja izločkov iz različnih prenasičenih trdnih raztopin. S pomočjo elektronske mikroskopije (SEM) so bili določeni tipi nastalih izločkov.

Na osnovi rezultatov preiskav smo prišli do naslednjih zaključkov. S pomočjo DSC metode lahko dokaj podrobno zasledujemo kinetiko izločanja iz prenasičene trdne raztopine, v našem primeru pri zlitinah AlMg7,5 ter AlMg3Cu. Kinetika izločanja je razvidna iz tendence večanja količine sproščene energije na segrevalnih DSC krvuljah pri povečevanju ohlajevalne hitrosti zlitin in vse bolj prenasičeni trdni raztopini. Poleg tega temperatura pričetka izločanja izločkov pada ob povečanju prenasičenja trdne raztopine. Če izračunamo delež izločevalne energije opazimo, da se ta pri obeh preiskovanih zlitinah povečuje s prenasičenjem trdne raztopine. Pri primerjavi obeh zlitin med seboj lahko zaključimo, da baker v zlitini izločanje izrazito poveča. Z elektronsko mikroskopijo smo v zlitini AlMg7,5 našli izločke  $\text{Al}_3\text{Mg}_2$ , v zlitini Al-Mg3Cu pa izločke na osnovi aluminija z nekaj magnezija in bakra, katerih stehiometrija pa ni ustrezala stehiometriji podani v literaturi<sup>[5]</sup>.

## REFERENCES

- [<sup>1</sup>] ASM HANDBOOK (1991): *Volume 4, Heat Treating*. ASM International, The Materials Information Company.
- [<sup>2</sup>] ROMHANJI, E., POPOVIC, M., GLISIC, D., DODOK, R., JOVANOVIC, D. (2006): Effect of annealing temperature on the formability of Al-Mg4.5-Cu0.5 alloy sheets. *Journal of Materials Processing Technology*; Vol. 177, pp. 386-389.
- [<sup>3</sup>] WANG, S.C., STARINK, M.J. (2007): Two types of S phases precipitates in Al-Cu-Mg alloys. *Acta Materialia*; Vol. 55, pp. 933-941.
- [<sup>4</sup>] WANG, M.J., STARINK, N., GAO, N. (2006): Precipitation hardening in Al-Cu-Mg alloys revisited. *Scripta Materialia*; Vol. 54, pp. 287-291.
- [<sup>5</sup>] KOVARIK, L., MILLER, M.K., COURT, S.A., MILLS, M.J. (2006): Origin of the modified orientation relationship for S(S'')-phase in Al-Mg-Cu alloys. *Acta Materialia*; Vol. 54, pp. 1731-1740.
- [<sup>6</sup>] MEDVED, J., MRVAR, P. (2006): Thermal Analysis of Mg-Al Alloy. *Materials Science Forum*; Vol. 508, pp. 603-608.
- [<sup>7</sup>] LOJEN, G., ANŽEL, I., KNEISSL, A., KRIŽMAN, A., UNTERWEGER, E., KOSEC, B., BIZJAK, M. (2005): Microstructure of rapidly solidified Cu-Al-Ni shape memory alloy ribbons. *Journal of Materials Processing Technology*; Vol. 162-163, pp. 220-229.